

Structural and optical properties of nanostructured bismuth oxide

Reem Sami Ali

College of Science, Al-Mustanisriyah University, Baghdad, Iraq

E-mail address: reem1deema1@yahoo.com

ABSTRACT

Thin films of bismuth oxide have been prepared utilizing vacuum evaporation. XRD analysis reveal that all the films were tetragonal polycrystalline structure with a preferred orientation along (002) plane. SEM images indicate that the grain size fall in the category of nanosize. AFM results assure that the nanonstructure behavior of thin films. Optical studies show that these films have a direct transition with optical energy gap equal to 2.5 eV.

Keywords: thin films' bismuth oxide; optical properties; structural properties

1. INTRODUCTION

In recent years, increasing attention has been focused on bismuth oxide, which is one of the most important metal oxide semiconductor has large uses in many fields such as gas sensors, solid oxide fuel cells, optical coatings, metal-insulator-semiconductor (MIS) capacitor, microwave-integrated circuits, ceramics and catalysts, Also used in the manufacture of optical fiber, where he witnessed this area significant progress due to the production of a variety of high-quality optical fibers such as bismuth oxide fiber doped with erbium (Er) and highly nonlinear bismuth oxide fibers [1-3]. These applications because owning a bismuth oxide some characteristics as energy band gap of 2 to 3.96 eV, high refractive index of 2.3 at 633 nm, dielectric permittivity, high photoconductivity and significant photoluminescence. [4,5].

Five polymorphs of Bi_2O_3 , known as α -, β -, γ -, δ - and ω - Bi_2O_3 were reported, each one possesses different crystal structures and various electrical, optical and mechanical properties, β -phase (tetragonal) is n-type semiconductor with a band gap of 2.58 eV, and also the metastable phase that can be stabilized to exist at room temperature by doping with impurities such as niobium or tantalum. [6-9].

There are different techniques for the preparation of bismuth oxide films, including: chemical bath deposition (CBD) [10], chemical spray pyrolysis [11], sol-gel [12], reactive magnetron sputtering [13], thermal oxidation of vacuum evaporated bismuth films [14], etc.

The aim of the present work was to study and discuss the structural, surface morphological and optical properties of Bi₂O₃ thin films prepared by thermal oxidation of bismuth films in air.

2. EXPERIMENTAL

The vacuum evaporation system at low pressure (about 10⁻⁵ Torr) was used to evaporate the bismuth (purity 99.999 %) onto cleaned glass substrates, maintained at room temperature. Bismuth oxide has been prepared by thermal oxidation in air at a temperature of 130 °C for 10 minutes. The thickness of the obtained films was about 200 nm which calculated by the weight method.

The structural analysis by X-ray diffraction (XRD) was carried out on a Philips type PW 1050 diffractometer using Cu-K α radiation with a wavelength of 1.5406 Å. Surface morphology was examined using scanning electron microscope (SEM) type (VEGA I I SBH MS 12, operating voltage is 16.00 kv) and atomic force microscope (AFM) type (SPM, AA-3000, Angstrom Advanced Inc. USA).

The transmission and absorption spectra of Bi₂O₃ thin film was measured using UV-VIS spectrophotometer type (1650-1700, Shimadzu, Japan) in the wavelength range (400-900 nm).

3. RESULTS AND DISCUSSION

Figure 1 shows X-ray diffraction (XRD) spectrum of Bi₂O₃ thin film, it is clear that the film is polycrystalline in nature. The pattern can be indexed as a tetragonal β -Bi₂O₃ structure with lattice parameters of $a = 7.742 \text{ \AA}$, $c = 5.631 \text{ \AA}$, $Z = 4$ (JCPDS card no. 27-0050) and a space group $P\bar{4}2_1c$ (114). These results are in good agreement with published results [15,16]. The observed and standard 'd' values along with their relative intensities are listed in Table 1. The careful observation of this table shows that the obtained film consists of a single phase. The maximum intensity peak of Bi₂O₃ is observed corresponding to diffraction angle 31.7555°.

The average grain size is about 48.64 nm for the thin film as estimating from Scherrer equation.

Table 1. Comparison of observed and standard (JCPDS) 'd' values for Bi₂O₃ thin film.

d(Å) observed	d(Å) standard	I / I₁	(hkl)	Type
3.18108	3.19	81	201	β -Bi ₂ O ₃
2.93050	2.949	21	211	β -Bi ₂ O ₃
2.81557	2.815	100	002	β -Bi ₂ O ₃

Figure 2 shows magnification 1.00 kx (a) and 2.00 kx (b) SEM images of Bi₂O₃ thin film. From these images the film surface consists of a uniform distribution of nanostructured grains with an average grain size is about 78 nm.

I (CPS)

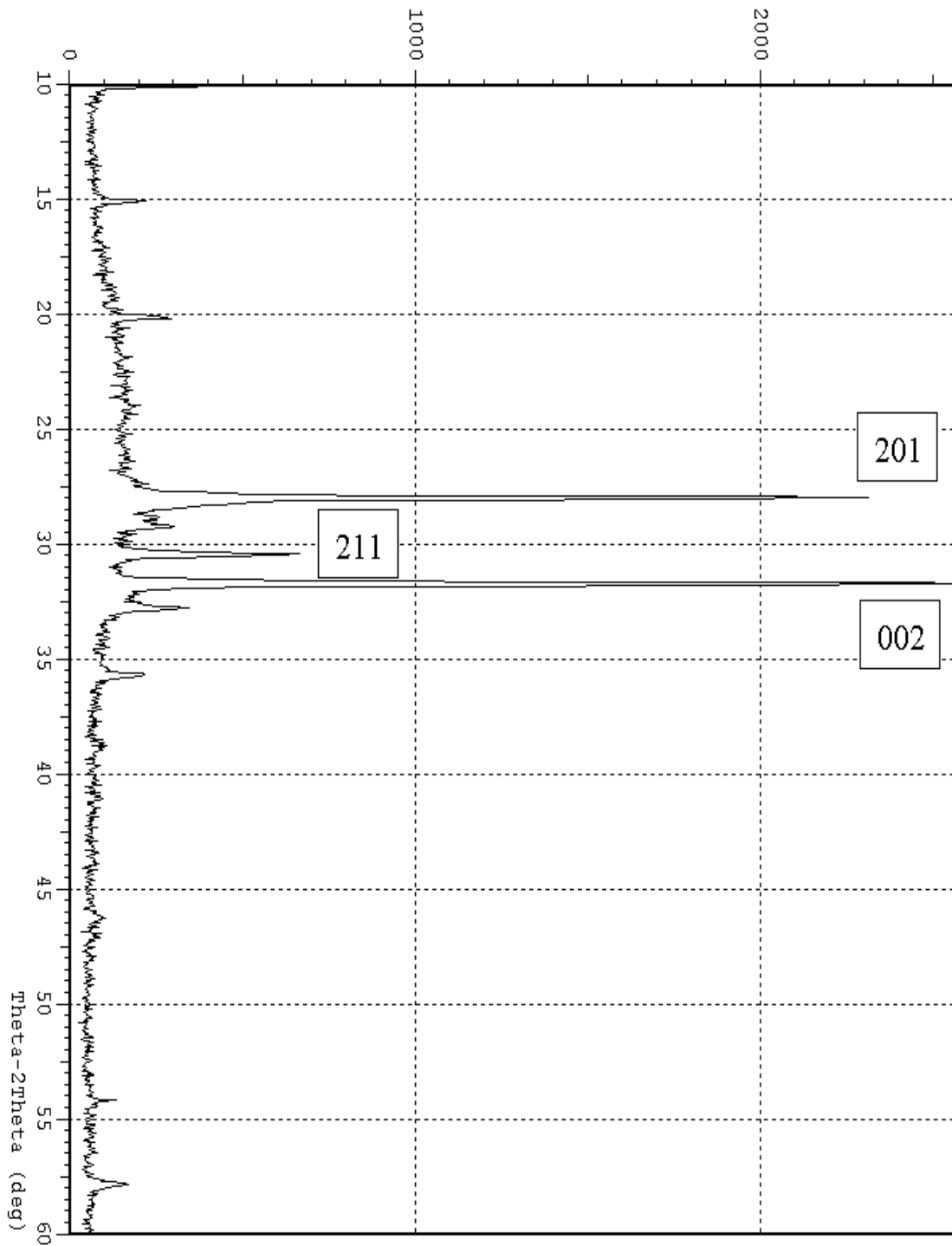
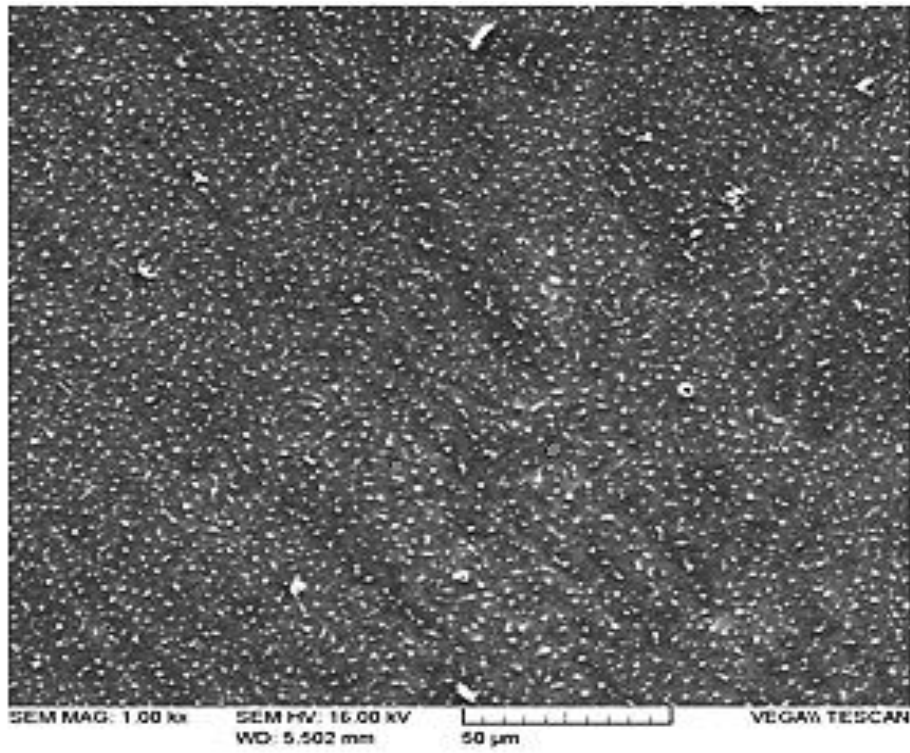
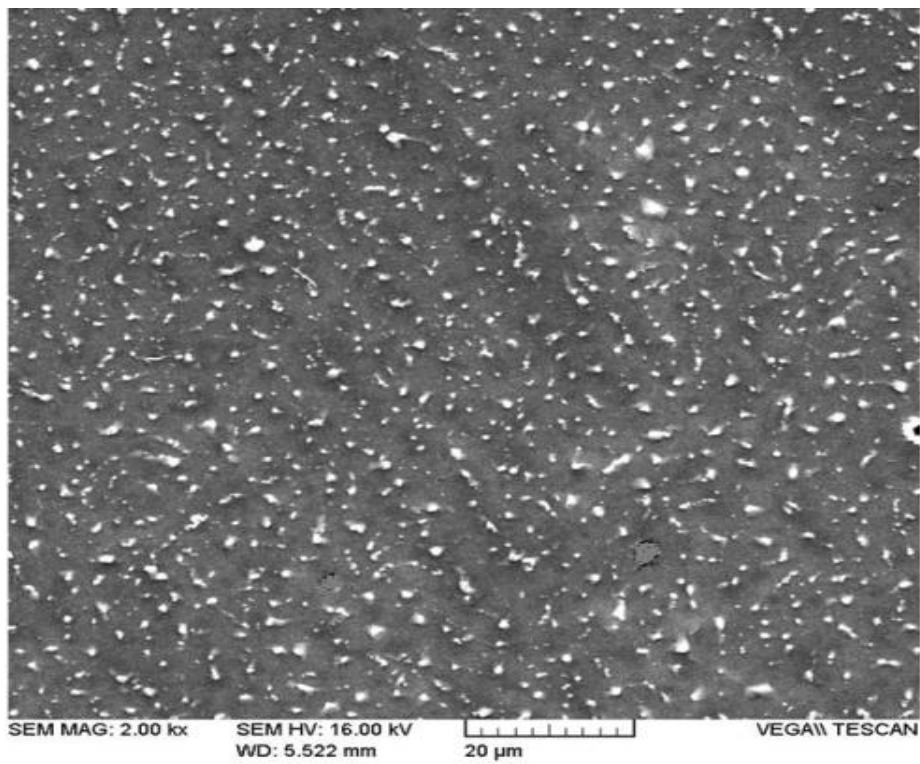


Fig. 1. XRD pattern of grown Bi_2O_3 film.



(a)



(b)

Fig. 2. MAG1.00 kx **(a)** and 2.00 kx **(b)** SEM images of Bi₂O₃ film.

Figure. 3 reveals the two-dimensional (a) and three dimensional (b) AFM images of Bi_2O_3 thin film. From this image, the average surface roughness and root mean square roughness values are 0.962 nm and 1.21 nm respectively, which indicated the smooth surface morphology of Bi_2O_3 . The average grain size deduced from AFM is about 81.57 nm was close to that estimated from SEM. Which indicate that the preparing films have a nanostructure.

The transmittance spectrum of bismuth oxide films deposited onto glass substrates are presented in Figure 4. One can see that the film shows good uniformity and transparency approximately (70-80 %) in the visible and NIR regions, and this high transmittance because there is no free electron (i.e. Electrons are linked to atoms by covalent bonds), this is because the breaking of electron linkage and moving it to the conduction band need photon with high energy [17].

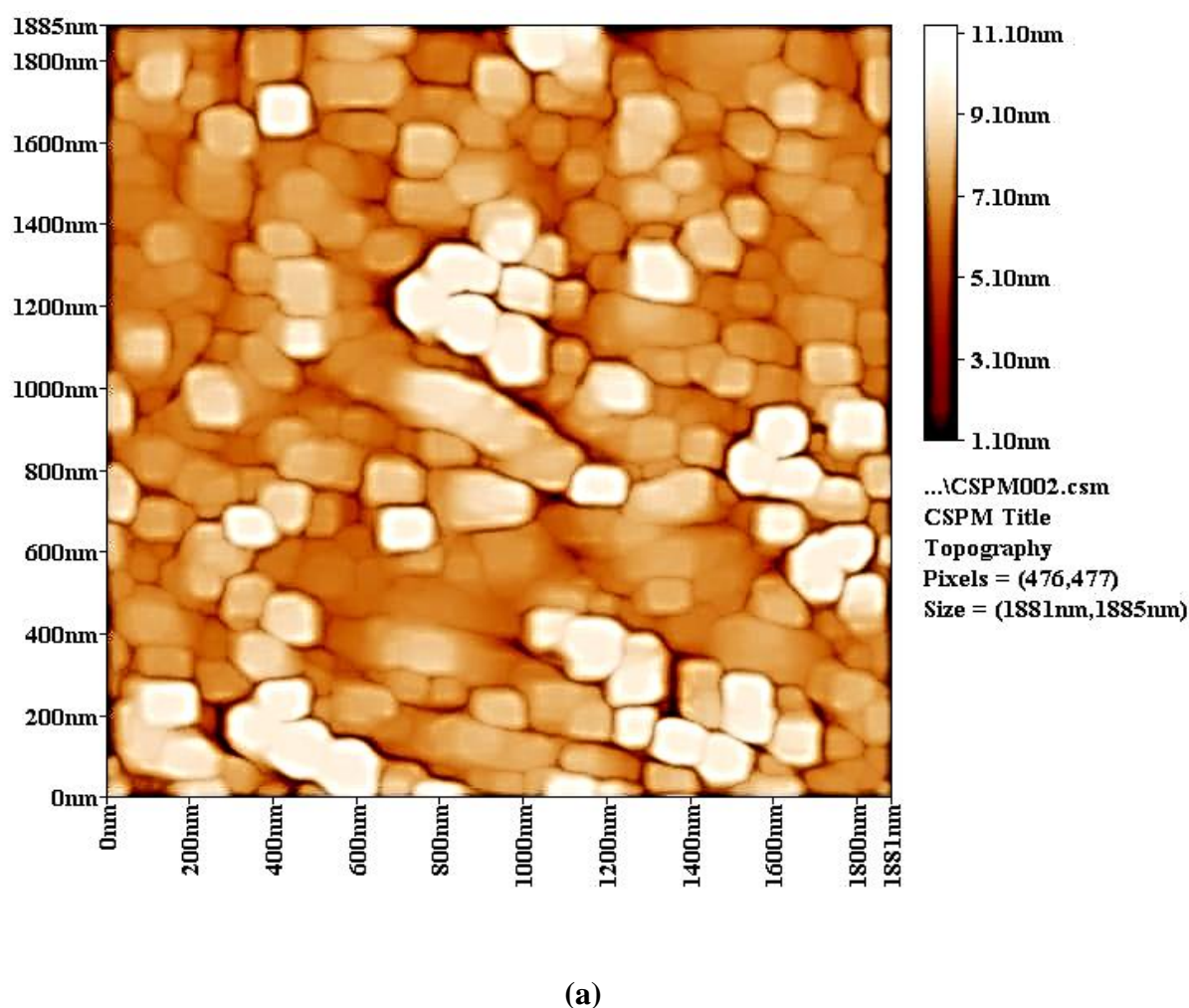
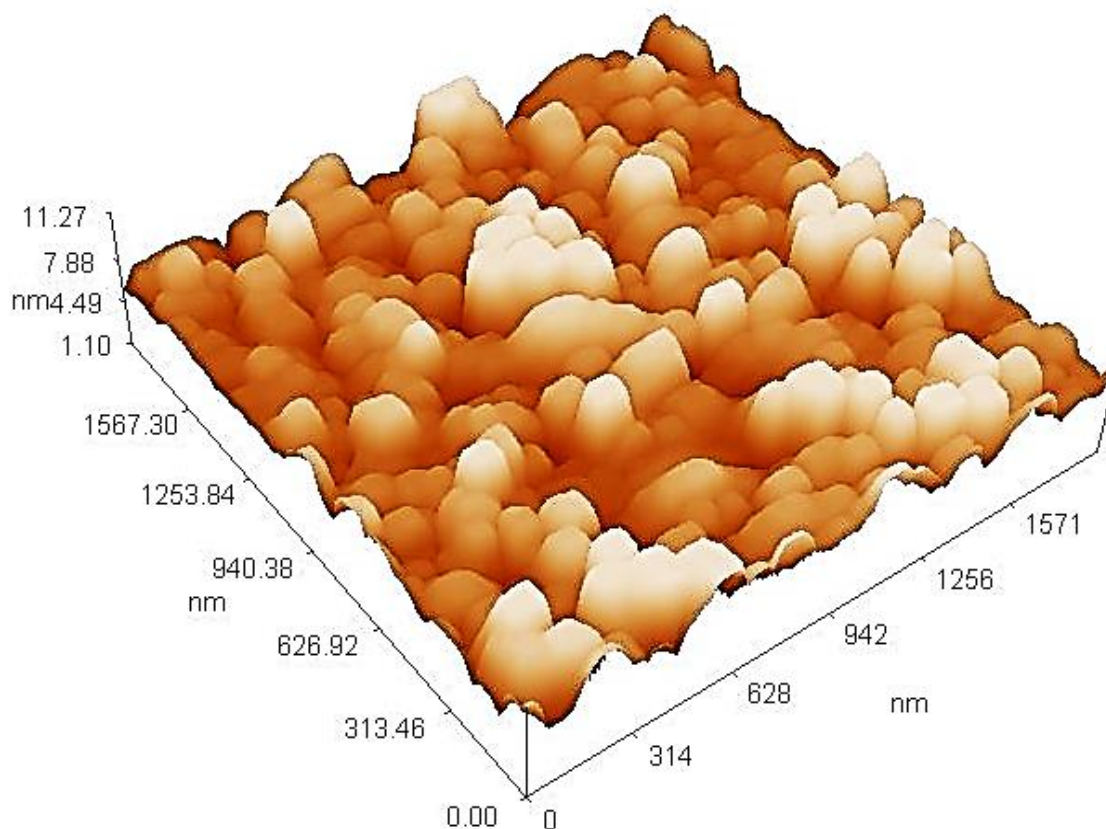


Fig. 3. Two-dimensional (a) and three-dimensional (b) AFM images of Bi_2O_3 film.



(b)

Fig. 3(continue). Two-dimensional (a) and three-dimensional (b) AFM images of Bi₂O₃ film.

Figure 5 shows the optical absorption spectrum of bismuth oxide films, it can be seen that absorption is low at high wavelengths (low energies) and then begins to increase with short wavelength (high energy), where the possibility of electron transitions be significant because of the incident photon energy be enough to move the electron from the valence band to the conduction band, the values of the absorption coefficient helps to conclude the nature of electronic transitions, according to the results in this figure, the coefficient of absorption for the Bi₂O₃ thin films is greater than 10⁴ cm⁻¹, this explains that the electron transition is direct, the energy and moment are maintained by the electrons and photons [17,18].

Figure 6 shows the plot of $(\alpha h\nu)^2$ versus $h\nu$, where α is the optical absorption coefficient and $h\nu$ is the energy of the incident photon. The energy gap (E_g) was estimated for a direct transition between valence and conduction bands from the expression [19]:

$$(\alpha h\nu) = K(h\nu - E_g)^{1/2}$$

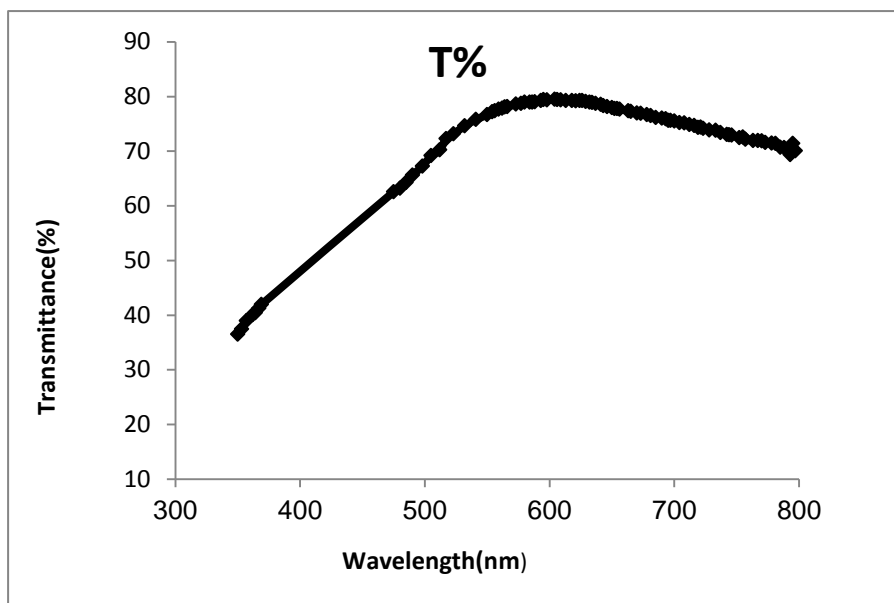


Fig. 4. Transmittance spectrum of Bi_2O_3 film.

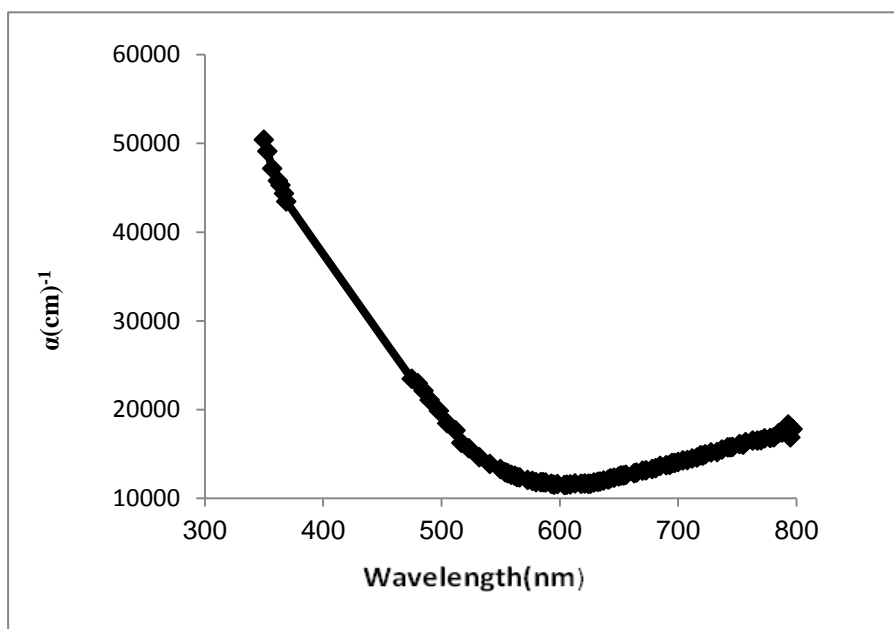


Fig. 5. Absorption spectrum of Bi_2O_3 film.

where K is a parameter, E_g is determined by extrapolating the straight line portion of the spectrum to $\alpha = 0$. From this drawing, the optical energy gap $E_g = 2.5$ eV is deduced and this value is close to the previously reported value [20,21]. One can notice that This energy gap is rather large for a photovoltaic cell, but should be ideal for photocatalytic water splitting [15].

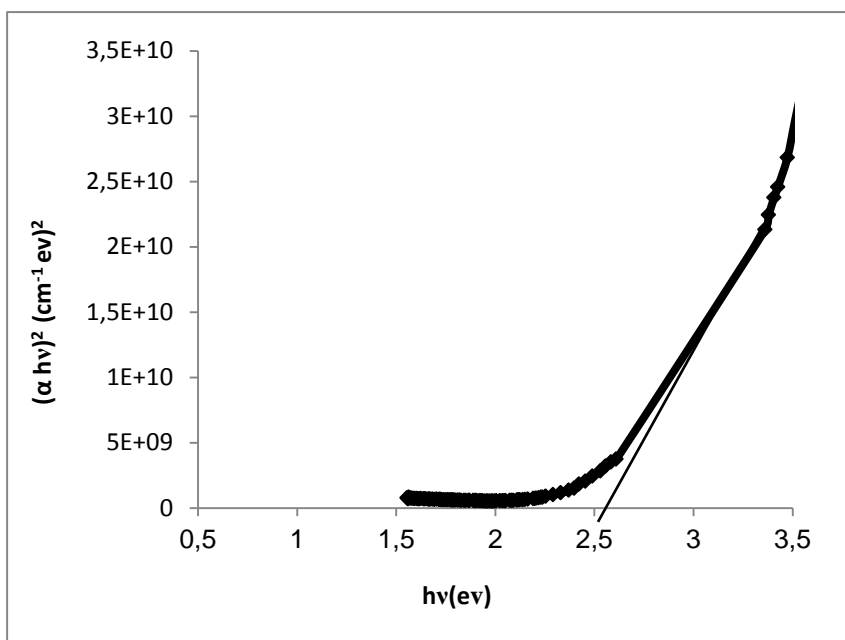


Fig. 6. Plots of $(\alpha hv)^2$ versus hv of Bi_2O_3 film.

4. CONCLUSIONS

Bismuth oxide was prepared successfully by the vacuum evaporation technique. The XRD analysis indicates that all the films were polycrystalline in nature. SEM images were homogenous showing a nanocrystalline structure which agrees with the AFM results which found that the average grain size was about 81.57 nm. The optical measurements show a direct transition with an optical band gap of 2.5 eV.

References

- [1] E. Öztürk, N. O. Kalaycioglu, S. Dayan, H. Ozlu, *Bull. Mater. Sci.* 36 (2013) 491-494.
- [2] S. W. Kang, S. W. Rhee, *Thin Solid Films* 468 (2004) 79-83.
- [3] C. M. Bedoya, M. J. Pinzón, J. E. Alfonso, E. R. Parra, J. J. Olaya, *Dyna* 79 (2012) 139-148.
- [4] J. In, I. Yoon, K. Seo, J. Park, J. Choo, Y. Lee, B. Kim, *Chem. Eur. J.* 17 (2011) 1304-1309.
- [5] S. Condurache-Bota, G. I. Rusu, N. Țigău, R. Drașovean, C. Gheorghieș, *Rev. Roum. Chim.* 54 (2009) 205-211.
- [6] H. T. Fan, S. S. Pan, X. M. Teng, C. Ye, G. H. Li, L. D. Zhang, *Thin Solid Films* 513 (2006) 142-147.
- [7] S. Park, S. An, H. Ko, C. Jin, and C. Lee, *Bull. Korean Chem. Soc.* 33 (2012) 3368-3372.

- [8] L. Leontie, M. Caraman, M. Alexe, C. Harnagea, *Surf Sci* 507-510 (2002) 480-485.
- [9] A. J. Salazar-Pérez, M. A. Camacho-López, R. A. Morales-Luckie, V. Sánchez-Mendieta, F. Ureña-Núñez, J. Arenas-Alatorre, *Superficies y Vacío* 18 (2005) 4-8.
- [10] T. P. Gujar, V. R. Shinde, C. D. Lokhande, R. S. Mane, S. -H. Han, *Appl Surf Sci* 250 (2005) 161-167.
- [11] V. V. Killedar, C. H. Bhosale, C. D. Lokhande, *Tr. J. Phys* 22 (1998) 825-830.
- [12] M. Gotić, S. Popović, S. Musić, *Mater Lett* 61 (2007) 709-714.
- [13] P. Lunca Popa, S. Sønderby, S. Kerdsonpanya, J. Lu, N. Bonanos, P. Eklund, *J. Appl. Phys.* 113 (2013) 046101.
- [14] S. Patil, V. Puri, *Arch. Appl. Sci. Res.* 3 (2011) 14-24.
- [15] J. Morasch, S. Li, J. Brötz, W. Jaegermann, A. Klein, *Phys. Status Solidi A* 211 (2014) 93-100.
- [16] Gopinath P., Chandiramouli R., *Res. J. Pharm. Biol. Chem. Sci.* 4 (2013) 8-14.
- [17] M. Dahshan, "Introduction to Material Science and Engineering", 2nd Ed, (2002).
- [18] B. Thangaraju, P. Kalianna, *Cryst. Res. Techno* 35 (2000).
- [19] S. M. Sze, "Physics of Semiconductor Device", 3rd Ed, John Wiley (2007).
- [20] Hashim A. R. Zalzal, Basheer Y. Muhson, Muhnad A. Ahmed, *Journal of Al-Nahrain University* 15 (2012) 80-82.
- [21] R. A. Ismail, *Journal of Semiconductor Technology And Science* 6 (2006) 119-123.

(Received 18 May 2014; accepted 26 May 2014)